

Mechanical strength and coordination defects in compressed silica glass: Molecular dynamics simulations

Yunfeng Liang,^{1,3} Caetano R. Miranda,^{2,3} and Sandro Scandolo^{2,3}

¹*International School for Advanced Studies (SISSA), Via Beirut 2-4, 34014 Trieste, Italy*

²*The Abdus Salam International Centre for Theoretical Physics (ICTP), Strada Costiera 11, 34014 Trieste, Italy*

³*CNR-INFN/Democritos, National Simulation Center, 34014 Trieste, Italy*

(Received 7 November 2006; revised manuscript received 20 December 2006; published 11 January 2007)

Contrary to ordinary solids, which are normally known to harden by compression, the compressibility of SiO₂ (silica) glass has a maximum at about 2–4 GPa and its mechanical strength shows a minimum around 10 GPa. At this pressure, the compression of silica glass undergoes a change from purely elastic to plastic, and samples recovered from above 10 GPa are found to be permanently densified. Using an improved, *ab initio* parametrized interatomic potential for SiO₂ we provide here a unified picture of the compression mechanisms based on the pressure-induced appearance of unquenchable fivefold defects. By means of molecular-dynamic simulations we find them to be responsible for the reduction of the mechanical strength and for permanent densification. We also find that the compressibility maximum does not require changes of the tetrahedral network topology.

DOI: [10.1103/PhysRevB.75.024205](https://doi.org/10.1103/PhysRevB.75.024205)

PACS number(s): 61.43.Fs, 62.20.Qp, 62.50.+p

I. INTRODUCTION

Network-forming materials such as the amorphous forms of ice and silica, have been for a long time known to display a number of structural, dynamical, and mechanical anomalies, that models and experiments are only recently starting to interpret based on fundamental atomistic processes. Changes in bond lengths, network topology, and atomic coordination resulting from the application of pressure provide an ideal testing ground for atomistic models. In the case of silica (SiO₂) glass, compression leads to an unexpected mechanical weakening, with a reported minimum of the yield strength around 10 GPa¹ where the mechanical response changes from purely elastic to plastic, as first noted by Bridgman.² Samples recovered from pressures lower than 10 GPa appear indistinguishable from the original material, while compression above 10 GPa results in the recovery of a densified amorphous polymorph, with densities 10–20 % higher than the density of the starting material.^{2–7} The compressibility of silica glass in the elastic region below 10 GPa is also anomalous, as it shows a maximum at about 2–4 GPa.^{8–13} Despite the large pressure difference between the onset of the two anomalies, microscopic theories have traditionally attempted to explain both anomalies with a single model, typically consisting in the pressure-induced appearance of coordination defects triggering the activation of local rebonding events.^{14–17} In particular, local displacive mechanisms involving sixfold coordinated Si defects have been proposed earlier on as an effective microscopic path to compression and densification.¹⁸ Such models are seriously questioned however, by the lack of evidence for coordination defects below 8–10 GPa (i.e., where the compressibility anomaly takes place), in NMR,²¹ x-ray diffraction,²² Raman,^{23,24} and infrared spectroscopy²⁵ experiments. Moreover, most of the models proposed so far for densified glass obtained from cold decompression at room temperature,^{14,15,26} contain sizable amounts of coordination defects, which are also not seen in experiments.^{11,27} In order

to overcome this problem, models have been introduced, which explicitly forbid coordination changes. While some of these models correctly reproduce the compressibility maximum,¹³ they obviously cannot account for the cold densification process, as this is known to be crucially affected by coordination defects.^{22–25} More recently, an improved three-body potential has been successfully used to reproduce the elastic-to-plastic transition in shocked glass,²⁸ however, more than 95% of the Si atoms were reported to be still in fourfold coordination at pressures exceeding 20 GPa, which is in contrast with the experimental observation of substantial coordination changes above 10 GPa.²² Here we provide, using an *ab initio* parametrized interatomic potential for SiO₂, a unified theoretical model based on the pressure-induced appearance of fivefold coordinated silicon above 8–10 GPa, which describes all the observed phenomenology. In Sec. II we present the method, in Sec. III we discuss our findings, and in Sec. IV we summarize the results.

II. COMPUTATIONAL METHODS

Previously employed atomistic models for SiO₂ have been shown to be unable to reproduce the pressure-induced coordination changes found in *ab initio* molecular-dynamic simulations of liquid SiO₂.^{19,20} In this work we use a potential that was recently developed for silica,²⁰ which describes experimental data on most SiO₂ low-pressure crystalline polymorphs better than any other empirical model.^{29,30} With this potential we generated by molecular dynamics (MD) a glass sample consisting of 192 SiO₂ formula units by quenching a liquid configuration from 3000 down to 300 K at a rate of 14 K/ps. The MD time step was set to 0.72 fs (30 a.u.). We then analyzed the behavior of compressed glass by following two distinct routes: (i) by slow, cold compression at 300 K, at a rate of 0.3 GPa/ps, followed, at each pressure, by an equilibration time of 20 ps; and (ii) by repeating the quenching procedure from the liquid at selected pressures. The compression was performed using a variable-

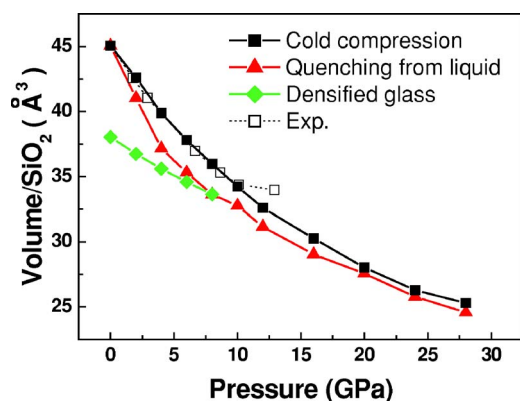


FIG. 1. (Color online) Equations of state of SiO_2 glass as obtained by cold compression (solid squares), isobaric quenching from the liquid (triangles), and cold decompression of a sample quenched from the liquid at 8 GPa (diamonds). Experimental data obtained by cold compression (empty squares) are from Ref. 10, using our value (2.23 g/cm^3) for the ambient pressure density (data in Ref. 10 are scaled to the ambient pressure volume). Error bars are equal or smaller than symbol sizes.

cell, constant-pressure algorithm,³¹ and temperature was controlled by means of a Nosé thermostat.³²

III. RESULTS AND DISCUSSION

In Fig. 1 we show the densities obtained as a function of pressure for the two compression protocols. Error bars for cold compression were evaluated by decreasing the compression rate between adjacent pressure points by up to ten times. Quenching rates from the liquid were instead found to be converged within the error bars of the cold compression run. The two compression mechanisms lead to different results for pressures below 10 GPa, but start to converge to similar structures and densities above 10 GPa. This indicates that below 10 GPa a “thermodynamical” minimum (within the realm of disordered phases) is not reached upon cold compression at least on the time scale of several tens of picoseconds. This is in agreement with experimental data,^{7,12,17} where temperature annealing is shown to be necessary to bring the system to a state of higher density and, presumably, lower enthalpy, at pressures below about 10 GPa. Experiments also indicate that the kinetics to reach thermodynamic equilibrium has a faster rate for increasing pressure,^{12,17} in agreement with our finding that at 10 GPa the two compression routes start to converge to similar results.

A microscopic analysis of the average Si-O coordination number (Fig. 2) shows that the silicon coordination number deviates significantly from the ideal value of four, characteristic of a perfect tetrahedral network, only above 8–10 GPa, in agreement with experiments on compressed glass.^{22–25} We verified that the network topology also did not change, up to 8 GPa. Such a rigidity of the network explains the elastic recovery of the samples below the threshold pressure. We calculated the compressibility of the glass compressed up to 28 GPa, and found it to display a maximum at about 3–5 GPa (Fig. 3), in fair agreement with experimental data

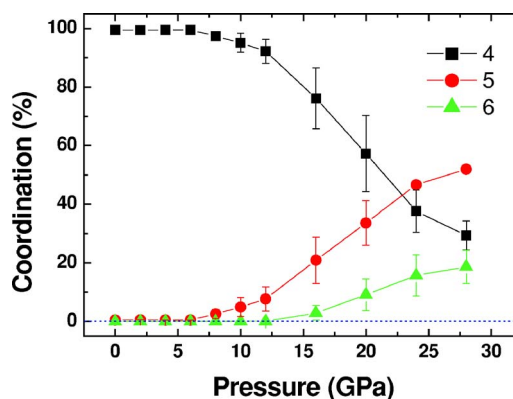


FIG. 2. (Color online) Percentages of Si atoms coordinated four (squares), five (circles), and six (triangles), to oxygen, as obtained by cold compression simulations (same results were obtained on samples quenched from the liquid). The cutoff distance for coordination was set to 2.1 Å and error bars were evaluated by changing the cutoff distance by $\pm 0.1 \text{ Å}$.

on the compressibility^{9,10,12} and on the sound velocity.¹¹ We therefore conclude that the compressibility maximum is not a consequence of a change in the network topology—as it would result, for example, in the case of an underlying kinetically hidden phase transition³³—nor of a change in Si coordination, as argued in Ref. 14. Rather, it is the consequence of a continuously increasing number of Si-O-Si plane-normal reversals (Fig. 4), as already suggested by Huang and Kieffer,¹³ and first hypothesized by Vukcevič.⁸ Such reversals can be interpreted¹³ as a continuous sequence of local reversible structural transitions similar to those which underlie the α -to- β transition in cristobalite. We also find that within the limits of our discrete pressure sampling no discontinuous phase transition takes place in the samples quenched from the liquid, in agreement with experiments on annealed samples,⁷ but in contrast with earlier experimental findings³⁴ as well as with the claims of Lacks,³⁵ which were,

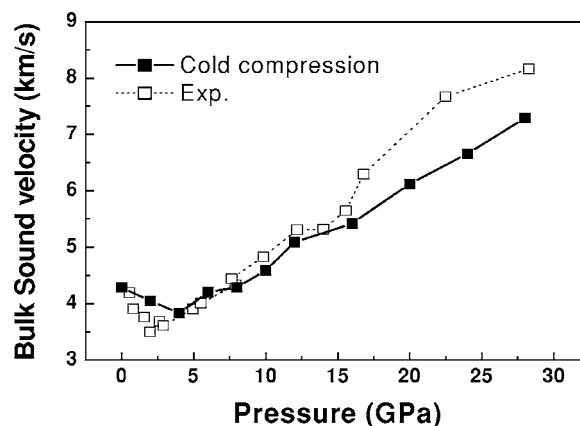


FIG. 3. Bulk sound velocity as a function of pressure as obtained by cold compression simulations. The bulk sound velocity v_s was calculated from the compressibility χ as $v_s = (\rho\chi)^{-1/2}$, where ρ is the density. The compressibility was determined by small (1–2 %) finite strains. Experimental data are from Ref. 11.

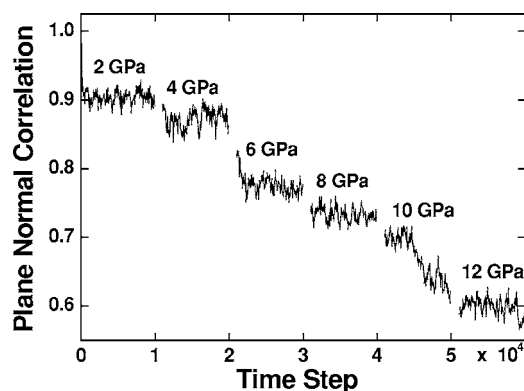


FIG. 4. The time-dependent average Si-O-Si plane normal correlation was calculated as in Ref. 13 by defining the vector normal $\hat{n} = \vec{R}_1 \times \vec{R}_2 / |\vec{R}_1 \times \vec{R}_2|$, with \vec{R}_1 and \vec{R}_2 the Si-O vectors in the Si-O-Si plane, and constructing the time-correlation function $C(t) = \langle \hat{n}(t) / \hat{n}(0) \rangle$, where the average $\langle \dots \rangle$ is taken over the different Si-O-Si in the sample. The time origin ($t=0$) coincides with the last configuration of the 0 GPa simulation. Pressure was increased in a stepwise fashion with steps of 2 GPa every 7 ps (10^4 steps). For increasing pressure, a continuously increasing number of Si-O-Si planes switch their plane orientation, as already observed in Ref. 13, leading to a decay of the correlation function.

however, based on cold compression simulations where the thermodynamical minimum cannot be reached.

Compression above 10 GPa results instead in important changes in the network topology and in irreversible densification. A similar elastic-plastic transition at around 9–10 GPa has been found also in shock-wave simulations.²⁸ Topological changes of the network are tightly connected with the appearance of fivefold Si-O coordination defects (see Fig. 2). The idea that coordination changes could be responsible for compression and densification of glasses above a critical pressure has been originally put forward by Stolper and Ahrens.¹⁸ They suggested a displacive mechanism leading to the spontaneous formation of sixfold coordinated Si, which—they argued—could provide a microscopic path to the network reorganization required to obtain a densified recovered sample. Our simulations show that sixfold coordinated Si only appears in significant amounts above 16–20 GPa, in agreement with infrared spectroscopy studies,²⁵ while coordination changes are found to be essentially fivefold between 10 and 16 GPa. We thus infer that the plastic behavior observed in glass above 10 GPa is a consequence of the pressure-induced appearance of fivefold defects. The presence of fivefold coordinated silicon has been reported in silicate glasses³⁶ and crystals³⁷ quenched from high pressure. Fivefold defects are also known to be responsible for the diffusivity maximum in silicate melts,³⁸ and they have been also advocated among the possible transition states in the atomic migration mechanisms responsible for the high-temperature growth of quartz from glass.³⁹ Here we propose that fivefold coordinated Si-activated diffusion is responsible for the minimum of the glass yield strength observed at about 10 GPa in mechanical-strength measurements.¹ In order to corroborate such a hypothesis, we carried out MD calculations of the yield strength of our

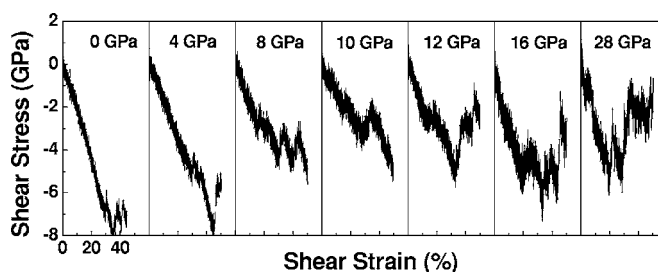


FIG. 5. Shear stress versus strain curves obtained by subjecting the samples to strain rates of 10^{10} s^{-1} at room temperature and different pressures.

samples by subjecting them to time-dependent shear strains, increasing at a constant rate, at different pressures.⁴⁰ Due to the intrinsic time-scale limitations of our MD approach, our strain rates, 1% per 1 ps, are much faster than any experimental rate. However, the stress-strain curves shown in Fig. 5 indicate not only a qualitative agreement with the position of the observed minimum of the yield strength, but also, quite surprisingly, with the absolute values of the yield strength, indicating that the microscopic processes responsible for the strength of compressed glass can be activated on the time scale of our MD simulations. However, it cannot be excluded that other long-term processes (longer than the time scale of our MD simulations) may also contribute to the observed minimum. Figure 6 shows that the plastic behavior is tightly correlated with the appearance of fivefold coordinated defects. Minimal sixfold coordination defects have been detected in the simulations of Fig. 6, indicating that octahedral units such as those proposed in Ref. 18 do not play any role in the plastic behavior of silica glass at the onset of densification. In order to support our speculation that fivefold defects drive the plastic events, we show in Fig. 7 the mean-squared displacement of Si atoms, separating the contribution due to Si atoms that have remained fourfold coordinated throughout the simulation from that due to Si atoms that have experienced a fivefold instantaneous coordination for at least one time step during the run. In order to remove the component of the elastic displacement due to the change in shape of the simulation cell we calculated all displacements in scaled coordinates, as defined in Ref. 31. By doing so we highlight the component of the atomic displacements due to internal elastic relaxation and/or to bond breaking and reforming, which is responsible for the plastic behavior. The results shown in Fig. 7 indicate that fivefold coordination enhances local rebonding and relaxation, and therefore plasticity.

The existence of fivefold coordination defects in silica glass is consistent with several experimental data. X-ray-diffraction experiments indicate that the Si-O bond length elongates starting from a pressure of about 8–10 GPa.²² Together with the lack of evidence for sixfold coordination below 17 GPa, from infrared experiments,²⁵ this implies the appearance of a sizable proportion of fivefold defects between 10 and 17 GPa. Moreover, our simulations show that the appearance of fivefold defects is accompanied locally by the formation of small rings in the network, with units similar to those reported in electronic structure calculations.⁴¹

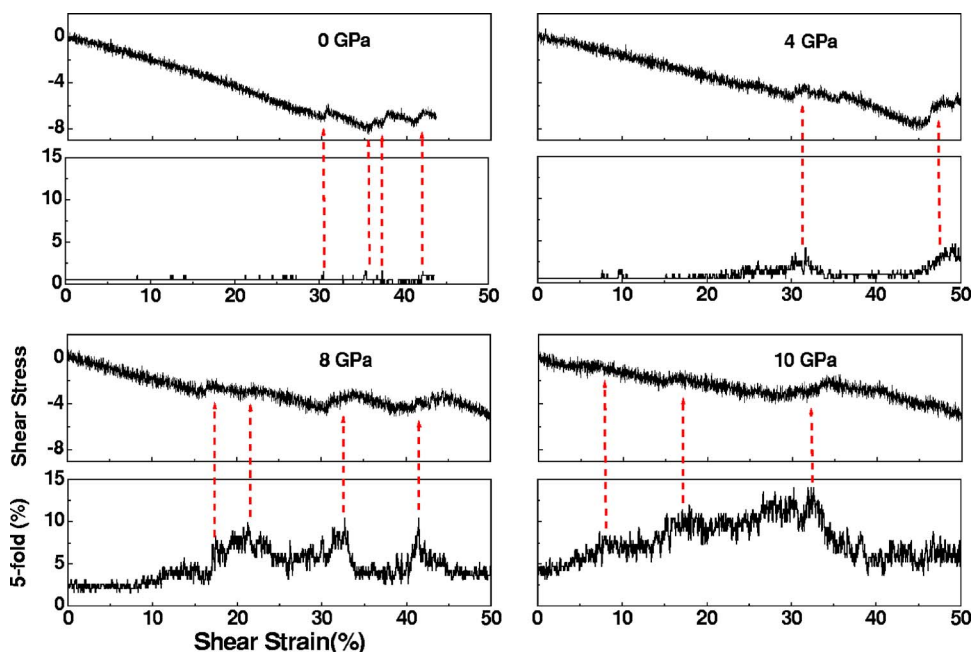


FIG. 6. (Color online) Percentages of fivefold coordinated silicon during the runs described in Fig. 5. The stress (in GPa) versus strain curves are those of Fig. 5 and are repeated here for clarity. Notice the peaks in the concentration of fivefold coordinated Si in connection with the onset of plastic events, as signaled by the sudden decrease of the shear stress. At 0 GPa the concentration of fivefold defects during such events is small but non-negligible (at least three simultaneous occurrences out of 192 Si atoms).

For example, the number of three-membered rings doubles between 10 and 16 GPa. Such an increase is consistent with the interpretation of *in situ* high-pressure Raman experiments.^{23,24} Finally, x-ray experiments on the analog system GeO₂ glass indicate that in the pressure window 6–10 GPa Ge is fivefold coordinated to oxygen on average.⁴² This could be equally accounted for by an equal proportion of fourfold and sixfold coordination, however.

Simulated glass samples recovered by cold compression from 10–28 GPa are found to have densities in very good agreement with experimental data on densified glass, as shown in Fig. 8. Both the threshold pressure and the range of densities agree well with the experimental data,^{4–7} as well as the fact that coordination defects disappear in the quenching process, leading to a dense but virtually defect-free

(within 1–2%) tetrahedral network, in agreement with Raman spectra.²⁷ It is important to stress that previous theoretical models for densified glass either contained unrealistically large concentrations of coordination defects,^{14,15,26} or had to be obtained by annealing,^{5,43} or by forcing fourfold coordination.^{5,43} The capability of our interatomic potential to produce a tetrahedral densified glass by following the experimental route, is a further illustration of its accuracy.

IV. SUMMARY

We find that the observed transition from elastic to plastic behavior observed in compressed glass, and responsible for glass permanent densification, is due to the appearance of fivefold coordinated Si defects above a threshold pressure of 8–10 GPa. Defects activate atomic diffusion and are respon-

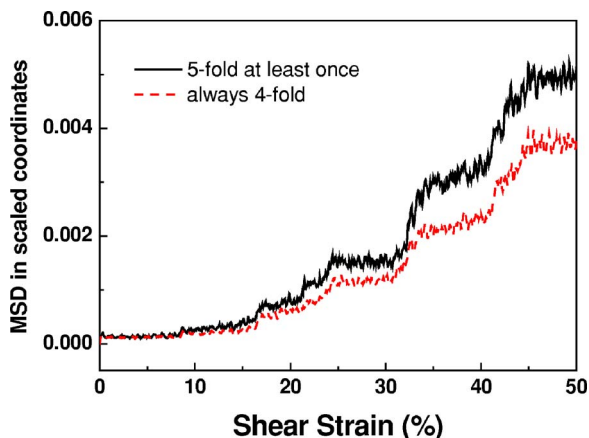


FIG. 7. (Color online) Mean-squared displacement (MSD) of silicon atoms in scaled coordinates during the run described in Fig. 5, at 8 GPa. Solid line: MSD averaged over those Si atoms that have been fivefold coordinated at least once during the run (75 atoms out of 192). Dashed line: MSD averaged over Si atoms always in fourfold coordination (117 out of 192).

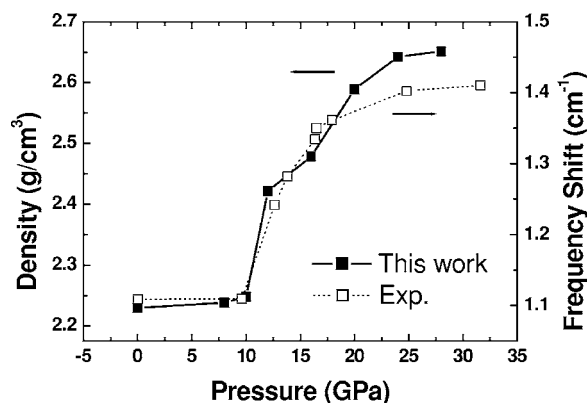


FIG. 8. Density of the simulated densified glass as obtained by ambient temperature decompression from different pressures. Direct measurements of densities are not available on a wide pressure range, so we compare our data with Brillouin frequency shifts, which are believed to be connected with density changes (Ref. 4).

sible for plastic behavior. NMR and x-ray-absorption spectroscopies would be ideally suited to verify our findings experimentally, but because fivefold defects are not quenchable to ambient conditions, experiments would have to be carried

out *in situ* at high pressure, which is not presently possible. Finally, we confirm that the compressibility anomaly is a purely elastic phenomenon that does not require topology changes or hidden phase transitions.

-
- ¹C. Meade and R. Jeanloz, *Science* **241**, 1072 (1988).
²P. W. Bridgman and I. Simon, *J. Appl. Phys.* **24**, 405 (1953).
³M. Grimsditch, *Phys. Rev. Lett.* **52**, 2379 (1984); *Phys. Rev. B* **34**, 4372 (1986).
⁴A. Polian and M. Grimsditch, *Phys. Rev. B* **41**, 6086 (1990).
⁵S. Susman, K. J. Volin, D. L. Price, M. Grimsditch, J. P. Rino, R. K. Kalia, P. Vashishta, G. Gwanmesia, Y. Wang, and R. C. Liebermann, *Phys. Rev. B* **43**, 1194 (1991).
⁶S. Sugai and A. Onodera, *Phys. Rev. Lett.* **77**, 4210 (1996).
⁷Y. Inamura, Y. Katayama, W. Utsumi, and K. I. Funakoshi, *Phys. Rev. Lett.* **93**, 015501 (2004).
⁸M. R. Vukcevich, *J. Non-Cryst. Solids* **11**, 25 (1972).
⁹K. I. Kondo, S. Lio, and A. Sawaoka, *J. Appl. Phys.* **52**, 2826 (1981).
¹⁰C. Meade and R. Jeanloz, *Phys. Rev. B* **35**, 236 (1987).
¹¹C. S. Zha, R. J. Hemley, H. K. Mao, T. S. Duffy, and C. Meade, *Phys. Rev. B* **50**, 13105 (1994).
¹²O. B. Tsiok, V. V. Brazhkin, A. G. Lyapin, and L. G. Khvostantsev, *Phys. Rev. Lett.* **80**, 999 (1998).
¹³L. Huang and J. Kieffer, *Phys. Rev. B* **69**, 224203 (2004).
¹⁴R. G. Della Valle and E. Venuti, *Phys. Rev. B* **54**, 3809 (1996).
¹⁵K. Trachenko and M. T. Dove, *J. Phys.: Condens. Matter* **14**, 7449 (2002).
¹⁶K. Trachenko and M. T. Dove, *Phys. Rev. B* **67**, 064107 (2003).
¹⁷K. Trachenko, M. T. Dove, V. Brazhkin, and F. S. El'kin, *Phys. Rev. Lett.* **93**, 135502 (2004).
¹⁸E. M. Stolper and T. J. Ahrens, *Geophys. Res. Lett.* **14**, 1231 (1987); R. Jeanloz, *Nature (London)* **332**, 207 (1988).
¹⁹A. Trave, P. Tangney, S. Scandolo, A. Pasquarello, and R. Car, *Phys. Rev. Lett.* **89**, 245504 (2002).
²⁰P. Tangney and S. Scandolo, *J. Chem. Phys.* **117**, 8898 (2002).
²¹X. Y. Xue, J. F. Stebbins, K. Masami, P. F. Mcmillan, and B. Poe, *Am. Mineral.* **76**, 8 (1991).
²²C. Meade, R. J. Hemley, and H. K. Mao, *Phys. Rev. Lett.* **69**, 1387 (1992).
²³R. J. Hemley, H. K. Mao, P. M. Bell, and B. O. Mysen, *Phys. Rev. Lett.* **57**, 747 (1986).
²⁴C. H. Polsky, K. H. Smith, and G. H. Wolf, *J. Non-Cryst. Solids* **248**, 159 (1999).
²⁵Q. Williams and R. Jeanloz, *Science* **239**, 902 (1988).
²⁶L. V. Woodcock, C. A. Angell, and P. Cheeseman, *J. Chem. Phys.* **65**, 1565 (1976); J. S. Tse, D. D. Klug, and Y. Le Page, *Phys. Rev. B* **46**, 5933 (1992).
²⁷G. E. Walrafen and P. N. Krishnan, *J. Chem. Phys.* **74**, 5328 (1981); P. Mcmillan, B. Piriou, and R. Couty, *ibid.* **81**, 4234 (1984).
²⁸L. P. Davila, M. J. Caturla, A. Kubota, B. Sadigh, T. Diaz de la Rubia, J. F. Shackelford, S. H. Risbud, and S. H. Garofalini, *Phys. Rev. Lett.* **91**, 205501 (2003); A. Kubota, M. J. Caturla, J. S. Stolken, and M. D. Feit, *Opt. Express* **8**, 611 (2001).
²⁹D. Herzbach, K. Binder, and M. H. Müser, *J. Chem. Phys.* **123**, 124711 (2005).
³⁰Y. F. Liang, C. R. Miranda, and S. Scandolo, *J. Chem. Phys.* **125**, 194524 (2006).
³¹M. Parrinello and A. Rahman, *Phys. Rev. Lett.* **45**, 1196 (1980).
³²S. Nosé, *Mol. Phys.* **52**, 255 (1984).
³³K. H. Smith, E. Shero, A. Chizmeshya, and G. H. Wolf, *J. Chem. Phys.* **102**, 6851 (1995).
³⁴G. D. Mukherjee, S. N. Vaidya, and V. Sugandhi, *Phys. Rev. Lett.* **87**, 195501 (2001).
³⁵D. J. Lacks, *Phys. Rev. Lett.* **84**, 4629 (2000).
³⁶J. F. Stebbins, *Nature (London)* **351**, 638 (1991).
³⁷J. F. Stebbins and B. T. Poe, *Geophys. Res. Lett.* **26**, 2521 (1999); R. J. Angel, N. L. Ross, F. Seifert, and T. F. Fliervoet, *Nature (London)* **384**, 441 (1996).
³⁸C. A. Angell, P. A. Cheeseman, and S. Tamaddon, *Science* **218**, 885 (1982).
³⁹M. J. Aziz, S. Circone, and C. B. Agee, *Nature (London)* **390**, 596 (1997).
⁴⁰See, e.g., M. F. Horstemeyer, M. I. Baskes, and S. J. Plimpton, *Acta Mater.* **49**, 4363 (2001).
⁴¹N. S. O. Ekunwe and D. J. Lacks, *Phys. Rev. B* **66**, 212101 (2002).
⁴²M. Guthrie, C. A. Tulk, C. J. Benmore, J. Xu, J. L. Yarger, D. D. Klug, J. S. Tse, H.-K. Mao, and R. J. Hemley, *Phys. Rev. Lett.* **93**, 115502 (2004).
⁴³L. Huang and J. Kieffer, *Phys. Rev. B* **69**, 224204 (2004).